

Phase transition in LiVO_2 studied by near-edge x-ray-absorption spectroscopy

H. F. Pen, L. H. Tjeng, E. Pellegrin, F. M. F. de Groot, and G. A. Sawatzky
*Laboratory of Solid State Physics, Materials Science Centre, University of Groningen,
 Nijenborgh 4, 9747 AG Groningen, The Netherlands*

M. A. van Veenendaal
European Synchrotron Radiation Facility, Boîte Postale 220, F-38043 Grenoble Cédex, France

C. T. Chen*
AT&T Bell Laboratories, Murray Hill, New Jersey 07974
 (Received 15 November 1996; revised manuscript received 5 February 1997)

We present temperature-dependent V-2*p* and O-1*s* x-ray-absorption spectra of LiVO_2 . The aim of this study is to monitor changes in electronic structure on going through the phase transition. The spectral changes turn out to be very small: the V-3*d*-O-2*p* hybridization does not change considerably, and the symmetry of the V-ion ground state (high-spin 3T_1) is retained. To explain our results, together with the anomalously low magnetic susceptibility below the transition temperature, we propose a model in which a three-orbital sublattice is formed in the V (111) planes, which results in a total singlet state. [S0163-1829(97)00623-1]

I. INTRODUCTION

In this paper, we present an x-ray-absorption spectroscopy (XAS) study of the changes in the local electronic structure at the phase transition in LiVO_2 . Through the years, vanadium oxides have attracted much attention because of their interesting electronic and magnetic properties. In many vanadium oxides, phase transitions occur as a function of temperature or pressure. By far the most famous example is V_2O_3 , showing a metal-insulator transition¹ with a conductivity change of a factor of 10^7 , whose origin is still controversial after 50 years. Though less extensively studied, the phase transition in LiVO_2 also is very interesting because of the peculiar magnetic behavior,² and in the literature several explanations³⁻⁶ have been proposed. We will show that our temperature-dependent XAS studies provide useful information concerning the electronic structure, and discuss the results in the light of the proposed transition mechanisms.

LiVO_2 has an ordered rocksalt structure with Li, V, and O occupying alternating (111) cubic planes.⁷ Because the Li layers are highly ionic, the material can be regarded as quasi-two-dimensional, with V^{3+} (d^2) ions forming two-dimensional (2D) hexagonal layers. LiVO_2 exhibits a first order phase transition² at around $T_t = 500$ K, with a peculiar change in magnetic properties. Above T_t , the compound is paramagnetic, showing a Curie-Weiss susceptibility $\chi \propto C/(T + \Theta)$ with a very large negative $\Theta = -1800$ K, corresponding to a large antiferromagnetic coupling. Below T_t , a virtually nonmagnetic phase is present, with no sign of long range magnetic order, and with a very low residual susceptibility attributed to V^{4+} impurities. The material remains semiconducting in both phases.⁸

A very obvious mechanism for the phase transition is the occurrence of a high-spin-low-spin transition at T_t due to a crystallographic distortion. For LiVO_2 this mechanism has not been discussed in the literature yet, but it is thought to be the driving force of the phase transition in, e.g., LaCoO_3

(Refs. 9 and 10). Above T_t , each V ion is surrounded by six oxygen ions in, approximately, O_H symmetry: this splits the 3*d* states in a threefold degenerate t_{2g} and a doubly degenerate e_g^σ level. In the low-temperature phase the symmetry is lowered to C_{3v} and the t_{2g} splits into an a_1 and a doubly degenerate e_g^π level. In the case that the a_1 level is lower in energy and the distortion is large, the trigonal component of the crystal field splitting, $\Delta_t = E(e_g^\pi) - E(a_{1g})$, could be large enough to overcome the Hund's rule exchange energy J_H . In this case, the local magnetic moment would be quenched and a nonmagnetic state would occur.

A more subtle explanation was proposed by Goodenough:³ because of the trigonal lattice distortion below T_t , with an increase in the c/a ratio,¹¹ he attributed the anomalously low susceptibility to the formation of trimers. The nonmagnetic behavior would be due to molecular orbital (MO) formation in the basal plane leading to a singlet ground state. The transition was attributed to the comparable size of the bandwidth W and the Coulomb repulsion energy U (Ref. 12). The condition $W \approx U$, related to a critical metal-metal distance R_c , would imply a lattice instability, with a crossover from a localized ($W < U$) to a delocalized regime ($W > U$) on decreasing the temperature through T_t . If we would go to the uncorrelated MO limit, i.e., $W \gg U$, it is obvious that a triangle with six electrons would form an $S = 0$ ground state. In this limit also the local spin would be quenched.

The assumed formation of trimers is supported by x-ray diffraction data by Cardoso,¹³ which shows weak superlattice reflections below T_t corresponding to a supercell with $a' = \sqrt{3}a$. Also recent extended x-ray-absorption fine structure¹⁴ and ${}^{51}\text{V}$ NMR (Ref. 15) studies are consistent with a displacement of the V ions. On the basis of their NMR data, Onoda *et al.*^{5,6} pointed out that the phase transition would be best described as a spin Peierls like distortion into trimers. In this picture, a triangle of three spin triplet ions are

coupled in a nearest neighbor Heisenberg fashion. With an exchange constant between the spins in the cluster much larger than that between the spins in neighboring clusters, this would result in a total spin $S_{\text{tot}}=0$ ground state for the trimer.

In order to get more insight in the electronic structure of LiVO_2 and its changes on going through the phase transition, we studied the V-2*p* and O-1*s* spectra as a function of temperature. The O-1*s* spectrum gives information about the degree of V-3*d*-O-2*p* covalency, while the V-2*p* spectrum probes the local ground state symmetry of the V ion.

II. EXPERIMENTAL DETAILS

The XAS measurements were carried out at the AT&T Bell Laboratories ‘‘Dragon’’ high-resolution soft-x-ray beam line¹⁶ at the the National Synchrotron Light Source, Brookhaven. In this experiment, the energy resolution of the monochromator was approximately 0.15 eV. The energy scale was calibrated using NiO, for which the O-1*s* white line energy is known accurately from high-energy electron energy loss spectroscopy.¹⁷ The base pressure in the measuring chamber was 2×10^{-10} mbar. The x-ray-absorption was measured in the total electron yield mode and also in the fluorescence yield mode. The spectra were normalized to the total absorption intensity between 510 and 560 eV, after subtraction of a constant background ($\sim 20\%$ of the maximum absorption).

Polycrystalline samples of LiVO_2 were prepared in two steps. The starting materials V_2O_5 and Li_2CO_3 were mixed in demineralized water, with a molar ratio $\text{Li}/\text{V}=1.05$. After CO_2 was released, the light green solution was concentrated by evaporation and the residue was ground in an agate mortar. x-ray diffraction (XRD) measurements showed that the powder consisted mainly of LiVO_3 , with a small content of Li_3VO_4 . The material was pressed into pellets and reduced in flowing H_2 at 1073 K. From 673 K to 1073 K, the temperature was increased slowly (1 K/min) to prevent melting of the starting material. The total reaction time was 24 h. According to XRD the reaction product was a single phase LiVO_2 . After preparation, the samples were stored in argon atmosphere to prevent degradation by oxygen or water.

For the x-ray-absorption measurements, a sample was fixed on a copper plate using stainless steel strips. In order to obtain a clean surface, the sample was scraped *in situ* with a diamond file and annealed in 1 torr H_2 at 525 K for 1 h. This procedure is necessary to remove contaminants from the surface and to restore the stoichiometry of the surface. It is known that LiVO_2 is very air sensitive:¹⁸ on exposure to air, the surface is quickly oxidized and lithium is extracted from the bulk. However, this process can be reversed by annealing the material in H_2 (Ref. 18). The effectiveness of this cleaning procedure was verified by the fact that the O-1*s* x-ray-absorption spectrum taken using the relatively surface sensitive total electron yield method (with a probing depth of ~ 100 Å) is very similar to that using the bulk sensitive fluorescence yield technique (with a probing depth of ~ 2500 Å, Ref. 19). Although the fluorescence spectra are a good check for the sample quality, they are not very suitable for a detailed analysis, because of self-absorption effects. This leads to a distorted spectrum, in particular, at the V-

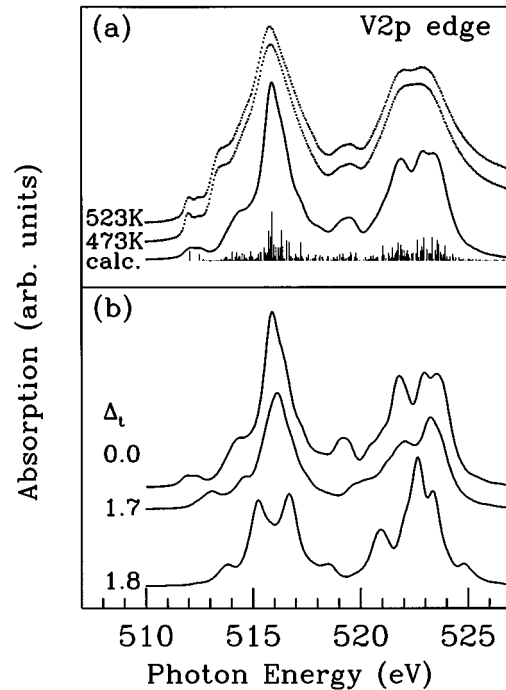


FIG. 1. (a) Total electron yield V-2*p* XAS spectra of LiVO_2 taken below and above T_t . The solid line and the sticks give the theoretical spectrum obtained from a cluster calculation. (b) Cluster calculations including a trigonal crystal field component Δ_t . The high- to low-spin transition occurs for $1.7 < \Delta_t < 1.8$ eV.

2*p* edge. The yield is reduced considerably, near-edge features appear more pronounced, and many details are lost. For this reason, we performed the temperature-dependent measurements discussed in the next section using the total electron yield mode.

The temperature-dependent measurements were carried out in steps of 25 K in the range 298–548 K. The heating cycle was repeated to ensure reproducibility of the spectra. The temperature was monitored by means of a thermocouple placed near the sample. After the experiment, the sample was checked by XRD. The XRD pattern appeared to be identical to that of the freshly prepared material; this precludes the possible formation of the LiV_2O_4 spinel phase due to non-stoichiometry, as observed by de Picciotto and Thackeray.²⁰

III. RESULTS AND DISCUSSION

A. Vanadium 2*p* XAS

Figure 1(a) shows the V-2*p* near-edge x-ray-absorption spectra below ($T=473$ K) and above T_t ($T=523$ K). Between 298 K and 473 K the spectra are virtually identical; however, between 473 K and 523 K (which includes T_t) small but clear changes occur. We note a small difference in the near-edge structure at 512 eV, and the appearance of a dip in the main L_2 peak (520–525 eV) above T_t , as if the spectrum becomes sharper. Because the changes appear to be reversible in subsequent temperature cycles, and because they occur only in a small temperature range around T_t , we attribute them to the phase transition. A temperature-dependent phonon broadening mechanism can be safely ex-

TABLE I. Parameters used in the cluster calculation of the V-2*p* and O-1*s* x-ray-absorption edges. All values are in eV. The charge transfer energy Δ is defined with respect to the lowest multiplet state.

$U=4$	$\Delta=4$	$Q=4$	$10Dq=1.3$
$(pd\sigma)=-2.2$	$(pd\pi)=1.1$	$(pp\sigma)-(pp\pi)=0.5$	

cluded because the spectrum for temperatures slightly above T_i is sharper than that for temperatures slightly below T_i .

The V-2*p* near-edge x-ray-absorption spectra are mainly determined by on-site V 2*p*→3*d* transitions. The main splitting into the L_2 (2*p*_{1/2}) and L_3 (2*p*_{3/2}) edge is due to the spin-orbit interaction of the 2*p* core hole. To interpret the experimental spectra, we carried out a cluster calculation which includes the full atomic multiplet theory, using a program developed by Thole *et al.*²¹ The model calculation involves a VO₆ cluster in O_H symmetry, and treats explicitly the strong hybridization between the V-3*d* and O-2*p* orbitals, as well as the on-site electron correlation effects.

The model has the following parameters as input: the O-2*p*-V-3*d* charge transfer energy Δ , the 3*d*-3*d* Coulomb repulsion U , the V-2*p*-V-3*d* Coulomb interaction Q , the O_H crystal field $10Dq$, and the Slater Koster integrals $(pd\sigma)$ and $(pd\pi)$ for the V-3*d*-O-2*p* hopping, and $(pp\sigma)$ and $(pp\pi)$ for the O-2*p*-O-2*p* hopping. Values for the parameters Δ , U , $(pd\sigma)$, and $(pd\pi)$ were estimated from experimental²² and theoretical²³ values for V₂O₃, a compound with similar V valence, V-O atomic distances, and local O coordination around the V ion. The spectrum depends on Q and U mainly by the presence of satellite structures for $Q \neq U$ (Ref. 24) at the high-energy side of the spectrum. Because these satellites are obscured by the O-1*s* edge in V compounds, we could not optimize the difference $Q-U$ and we took therefore $Q=U$. The various multiplet interactions are reduced to 80% of the atomic Hartree-Fock values to account for intra-atomic relaxation effects.²⁵ Only the O_H crystal field $10Dq$ is treated as an optimization parameter. The parameter values are listed in Table I.

The sticks in Fig. 1(a) show the theoretical transition probabilities. The solid line is the calculated spectrum, obtained by applying a Gaussian and Lorentzian broadening of 0.15 eV and 0.2 eV, to account for experimental resolution and lifetime, respectively. The calculated spectrum is in good agreement with the experimental spectra, especially for the high-temperature case, where a dip in the L_2 edge is present. The discrepancy between theory and experiment could be due to the state dependent lifetime broadening,^{26,27} which cannot be taken into account in a unique way. Due to the possibility of Coster-Kronig decay, the L_2 edge is broader than the L_3 ; also within the two main edges, the lifetime of the final states increases considerably with energy.

The most striking result of Fig. 1(a) is that both the high- and low-temperature spectra can be simulated very well by the same theoretical spectrum in which the ground state symmetry is the high spin 3T_1 . This indicates strongly that the phase transition is not accompanied by a symmetry change of the ground state. It is important to note here that an x-ray-absorption spectrum is very sensitive to the symmetry of the

ground state, because the absorption process is governed by dipole selection rules, which allow only a part of the possible final state $2p^53d^{n-1}$ multiplet intensities to be reached from the d^n ground state. So, if the ground state symmetry of the V ion would have changed, for instance, from high to low spin, then we would have seen quite a drastic change of the V-2*p* spectrum.

To illustrate this sensitivity of the technique to symmetry, we show in Fig. 1(b) first of all the result of the cluster calculation in the ionic limit, i.e., excluding the hybridization with O ligand states ($10Dq$ is increased to 1.8 eV, to partly compensate for the omitted covalency with the ligands). The ground state in the ionic limit is also high-spin 3T_1 . It can be clearly seen that this spectrum is very similar to the spectrum of the full cluster model, illustrating that symmetry is more important for the spectral line shape than hybridizational effects, even in strongly covalent V compounds. To simulate the questioned high- to low-spin transition, we now have to include a trigonal component Δ_t in the crystal field in our calculations. The results are shown in Fig. 1(b) for different values of Δ_t , where the high- to low-spin transition occurs for Δ_t between 1.7 and 1.8 eV. It is quite remarkable that the spectrum for a Δ_t value as large as 1.7 eV (high spin ground state) still has a resemblance to that for the undistorted O_H situation (i.e., $\Delta_t=0.0$ eV): despite the apparent differences in the spectra, most of the peaks and shoulders in the $\Delta_t=0.0$ eV spectrum can still be clearly recognized in the $\Delta_t=1.7$ eV spectrum. For the $\Delta_t=1.8$ eV case (low spin ground state), however, the spectrum is completely different: new peaks show up at quite different energies. A small change in Δ_t , from 1.7 to 1.8 eV, causes a sudden and drastic rearrangement of the spectral intensities. This demonstrates that the x-ray-absorption spectrum will not be essentially altered by a trigonal distortion, as long as the ground state symmetry is preserved. Based on the experimental observation that the changes in the x-ray-absorption spectrum are very small (see Fig. 1), we can safely conclude that the low susceptibility of LiVO₂ below T_i is definitely not due to a low-spin state. From a more theoretical point of view, such a high- to low-spin transition should also not be expected since this would require an unphysically large trigonal distortion. Because the low-spin spectrum is completely different from the high spin one, we can also conclude that the *d* electrons are still considerably localized. A large delocalization would lead to a mixing in of the low-spin configuration, which would strongly affect the V-2*p* spectrum.

In our view, the most plausible explanation for the changes in the V-2*p* spectra is a small change in the V-3*d*-3*d* hybridization. Above T_i , the atomic approximation is very good; this is also concluded from the high-temperature magnetic susceptibility, which is in agreement with a paramagnetic phase and a local spin moment close to the atomic value.¹¹ However, below the transition temperature, V-3*d*-3*d* hopping integrals are increased due to a shorter V-V distance, as pointed out by Goodenough.³ Nevertheless, the low-temperature spectrum is still in good agreement with the atomic multiplet calculation. Therefore we conclude that the formation of trimers does not lead to a strong change of the 3*d* electron localization. In other words, the on-site V-3*d*-3*d* Coulomb interactions remain much larger than the V-3*d*-3*d* hopping integrals.

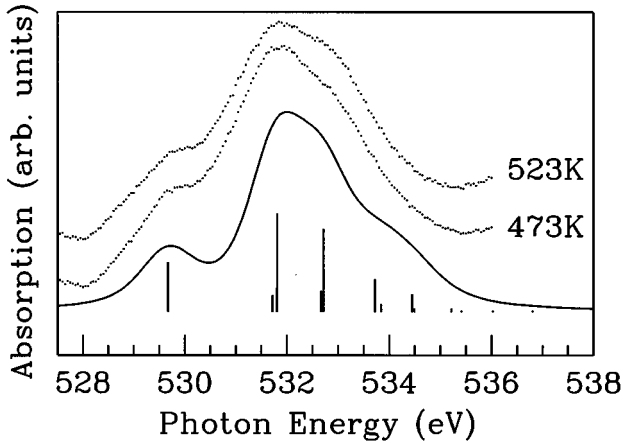


FIG. 2. (a) Total electron yield O-1s XAS spectra of LiVO_2 taken below and above T_c . (b) Near-edge region of the O-1s spectra, compared to a cluster calculation. The sticks indicate the theoretical transition probabilities.

Unfortunately, it is beyond our reach to calculate the V-2p spectrum for a V triangle. Nevertheless, we can argue that delocalization of the V-3d electrons would lead to significant changes in the V-2p XA spectrum, because configurations of different symmetries will mix into the ground state. In the extreme limit, i.e., complete delocalization into uncorrelated MO's, the weight of the 3T_1 symmetry configuration is strongly reduced: by projecting the MO wave function onto the atomic multiplet states,²⁸ one can show that this weight is only 3/16. Considering the large number of symmetry configurations contributing to the MO ground state, one can expect that the resulting spectrum is going to be very broad, probably similar to the 2p edge of metallic titanium or vanadium.²⁹ Certainly, it will be completely different from the 3T_1 spectrum from Fig. 1. Of course, we expect a gradual change in the V-2p XA spectrum on increasing the d-d hybridization (or the bandwidth W) with respect to U . Therefore, an absolute classification of the 3d electrons as being “localized” or “delocalized” is not possible from the XA spectrum only. Nevertheless, because of the apparent validity of the atomic multiplet approximation we believe that the V-3d electronic wave function is close to the localized limit.

B. Oxygen 1s XAS

Figure 2(a) shows the O-1s x-ray-absorption spectra below ($T=473$ K) and above ($T=523$ K) the transition temperature. The O-1s XA spectrum probes the unoccupied states of oxygen p character, because of the dipole selection rule and the local character of the x-ray-absorption process. The near-edge region, shown in Fig. 2, is attributed to states with mainly V-3d character, hybridized with O-2p states. The x-ray-absorption final state of the O $1s \rightarrow 2p$ transition appears to be less localized than that of the V $2p \rightarrow 3d$ transition. This gives rise to considerable dispersional broadening, leading to a spectral shape without much detail. As is the case for the V-2p edge, the differences in going through the phase transition are very small. The feature at 533 eV seems to be more pronounced above T_t .

Multiplets are also important for a correct description of the O-1s near-edge structure. To illustrate this, the experimental spectra are compared to the results of a model calculation on a VO_6 cluster in O_H symmetry, identical to that used above for the V-2p edge. Also the parameters used in the calculation are the same, see Table I. The sticks in Fig. 2 show that most of the essential features in the experimental spectra are well reproduced by the model calculation. The calculated line shape is obtained by convolution with a Gaussian and a Lorentzian, both of 0.8 eV full width at half maximum, in order to account for experimental resolution, dispersion, and lifetime. Although the relative contributions of the different effects are not accurately known, it is clear that the total broadening is much larger than for the V-2p spectra.

The lowest peak at 530 eV energy is assigned to transitions to the t_{2g}^3 (4A_2) final state. The other peaks can be attributed to transitions to doublet final states of t_{2g}^3 character, which appear at higher energy due to the on-site exchange interaction, and also to final states of $t_{2g}^2 e_g$ character. In a cluster calculation without Coulomb and exchange interactions, the calculated spectrum would have consisted of only two peaks, corresponding with transitions to t_{2g} and e_g unoccupied states, with an intensity ratio³⁰ of about 1:2. So multiplet effects push part of the t_{2g}^3 final states up in energy, which explains the low intensity of the 530 eV peak.

Because of the broadness of the spectrum, together with the number of parameters involved in the calculation, an analysis of the small temperature-dependent changes is not meaningful. However, the total spectral weight and the position of the shoulder with respect to the main peak do not change significantly. This means that the change in O-2p-V-3d hybridization and the change in ligand field strength are relatively small. The crystallographic distortion in LiVO_2 does not give rise to a strong energy redistribution of the V-3d states, in contrast with the case of VO_2 (Ref. 31).

C. Trimer model

From the analysis of the O 1s we conclude that V-O interactions do not change considerably, and are probably not a determining factor for the phase transition. The V-2p spectra show that the local spin moment at the V ion is $S=1$, both above and below T_t . A high-spin-low-spin transition can therefore be ruled out. The data seem to be consistent with the formation of V trimers,³ in which a triangle of three spin triplet ions are coupled in a nearest-neighbor Heisenberg fashion,^{5,6} resulting in a total spin $S_{\text{tot}}=0$ ground state for the trimer.

While the latter statement is true within the Heisenberg model, we would like to point out that the model itself should not be applied for a transition metal (TM) $3d^2$ system because it neglects completely the orbital degeneracy of the 3d states. In a localized system this orbital degeneracy will be lifted at low temperatures (the Jahn-Teller effect). This can lead to a structural phase transition, accompanied by a certain ordering of occupied orbitals. Such orbital ordering need not be driven by a lattice distortion; it can also be caused by magnetic exchange interactions.³² The strongest effects of this kind are observed in TM compounds with a

twofold e_g orbital degeneracy. Recently, it was shown³³ that also in TM compounds with a t_{2g} orbital degeneracy an orbital ordering is likely to occur, if the TM ions are in an approximately octahedral crystal field and ordered along the cubic (111) planes. In this type of structure, orbital ordering is a way to remove the magnetic frustration present in the triangular TM planes.

We will now discuss the arguments of Ref. 33 in some detail. Consider only the $3d(t_{2g})$ electrons in a degenerate Hubbard-type model, including on-site Coulomb (U) and exchange (J_H) interactions and nearest-neighbor hopping t . This means that we assume a system with a considerable degree of localization and a strong Hund's rule coupling. However, we allow for the threefold t_{2g} orbital degeneracy, which is one step beyond the Heisenberg model. Furthermore, we consider only σ overlap and neglect the much weaker π overlap. This implies that each orbital hybridizes with only two other nearest-neighbor orbitals: e.g., a d_{xy} orbital hybridizes with neighboring d_{xy} orbitals in the (110) and $(\bar{1}\bar{0})$ directions. This strongly nonuniform hybridization means that a strong antiferromagnetic exchange interaction can only be present between certain orbitals, i.e., those that have σ overlap. What is more, because of the orbital degeneracy, the exchange interactions also depend on the particular occupation of the t_{2g} orbitals. According to the Goodenough-Kanamori-Anderson rules,³ a strong antiferromagnetic interaction $J \propto t^2/U$ between orbitals is only present if both orbitals are singly occupied. Otherwise, the exchange interaction is weakly ferromagnetic or zero.

The highly nonuniform orbital hybridization, combined with the occupation dependent exchange, leads to an interesting observation. The frustration, which is present if one considers this system as a triangular Heisenberg antiferromagnet, can be removed by a certain orbital ordering. Take, for example, the ordering with the d_{yz} and d_{zx} orbitals singly occupied at all atoms. With all d_{xy} orbitals unoccupied, there is no AFM exchange along the (110) and $(\bar{1}\bar{0})$ directions. Because of the orbital ordering the effective AFM exchange interactions are only in four directions $[(101), (\bar{1}0\bar{1}), (011), \text{ and } (0\bar{1}\bar{1})]$ and no frustration is present. Another possible orbital ordering, which turns out to have the same mean field energy, is the one in which three orbital sublattices are formed. In the different sublattices either the d_{xy} , d_{yz} or the d_{zx} orbital is empty; the others are again singly occupied. This ordering leads quite naturally to the formation of three-site clusters, with a strong AFM interaction within the clusters and only weak exchange interactions between them.

To study the characteristics of such a three-site cluster and to verify if the proposed orbital ordering is also favorable on a local scale, an exact diagonalization study for three sites was carried out for different values of the d - d hopping integral t . It turned out that for small t the ground state has a total spin $S_{\text{tot}}=1$, with an orbital ordering as shown in Fig. 3(a). Above a critical value of t (t_c), a singlet ground state is obtained, with a different orbital ordering. In Fig. 3(b) it is shown that alternately the d_{xy} , d_{yz} , and d_{zx} orbitals are unoccupied, which is compatible with the proposed three-sublattice ordering. Therefore we conclude that this ordering is also favorable on a local scale, and that it leads to a non-

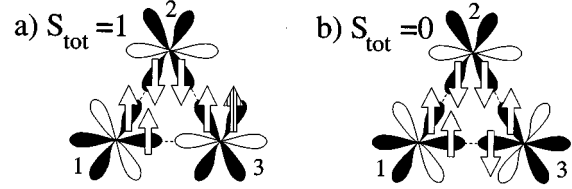


FIG. 3. Schematic configuration of the lowest triplet (a) and singlet (b) states in the exact diagonalization study. The spectator electron is hatched. Black and white shapes depict occupied and empty orbitals, respectively. Dashed lines represent σ bonds. Note that the wave function, depicted in (b) at site 3, is the $M_S=0$ component of a local $S=1$ state.

magnetic ($S_{\text{tot}}=0$) ground state. From a second order perturbation treatment, it can be shown that the triplet-singlet transition is due to the competition between Hund's rule exchange and kinetic energy; t_c is approximately proportional to J_H . In the $S_{\text{tot}}=1$ state, a "spectator" electron occupies a nonhybridizing orbital. With this ground state configuration, the virtually excited states still obey Hund's rule; however, in the lowest $S_{\text{tot}}=0$ state, all hybridizing orbitals are occupied, which turns the scale at large t .

At first sight, the concept of orbitally ordered trimers looks quite similar to the ideas discussed before. However, there are some subtle but important differences, related to the mechanism of the phase transition. Note that the three-sublattice orbital ordering is just a natural way to remove the magnetic frustration, even without a strong lattice distortion. A change from the $W < U$ to the $W > U$ regime¹² or the postulation of negligible intercluster exchange interactions^{5,6} does not seem essential: the magnetic decoupling of trimers follows directly from the orbital ordering. Interesting to note is the similarity between the occurrence of a critical value of t in the exact diagonalization of the three-site cluster, and the concept of a critical distance R_c for delocalization.¹² However, R_c is related to the Coulomb energy U via the condition $W \approx U$, while t_c depends on the Hund's rule exchange energy J_H . This reflects the difference between a crossover from a localized to a delocalized regime, and a transition between different orbital orderings. We note that the triplet-singlet transition was obtained for an isolated trimer and that the generalization of this calculation to the full lattice is far from straightforward. However, the concept of a $t_c \propto J_H$ separating different orbital orderings may be more general.

IV. CONCLUSIONS

In conclusion, we have obtained new information about the electronic structure and the phase transition of LiVO_2 by means of XAS. The spectra show that the V ions are in a high-spin 3T_1 state, not only above but also below T_t , i.e., that the local spin moment is retained on going through the phase transition. The validity of the atomic multiplet approximation in describing the V-2p spectra indicates a considerable degree of localization of the V-3d electrons, also below T_t . The data also indicate that the O-2p-V-3d hybridization hardly changes across T_t . We propose a mechanism which starts from the commonly accepted formation of triangular structures within the hexagonal V (111) planes,

and which assumes strong localization of the V-3d electrons. In a V triangle, the formation of a three-orbital sublattice can give rise to a total singlet state, which accounts for the anomalous low-temperature susceptibility in LiVO_2 .

ACKNOWLEDGMENTS

We thank R. H. Potze and F. ten Broek for assistance with the sample preparation and F. van der Horst for carrying out the x-ray-diffraction measurements. This investigation was supported by Stichting voor Fundamenteel Onderzoek der

Materie (FOM) with financial support from Nederlandse Organisatie voor Wetenschappelijk Onderzoek (NWO). The research of L.H.T. and F.M.F.d.G. has been made possible through the financial support of the Royal Netherlands Academy of Arts and Sciences. E.P. acknowledges financial support by the European Union under Contract No. SC1 CT91-0751. The National Synchrotron Light Source at Brookhaven National Laboratory is supported by the United States Department of Energy under Contract No. DE-AC02-76CH00016.

*Present address: Synchrotron Radiation Research Center, Hsinchu Science-Based Industrial Park, Hsinchu 300, Taiwan.

¹M. Foex, C. R. Acad. Sci. **223**, 1126 (1946).

²P. F. Bongers, Ph.D. thesis, University of Leiden, 1957.

³J. B. Goodenough, *Magnetism and the Chemical Bond* (Interscience, New York, 1963).

⁴T. A. Hewston and B. L. Chamberland, J. Solid State Chem. **65**, 100 (1986).

⁵M. Onoda, T. Naka, and H. Nagasawa, J. Phys. Soc. Jpn. **60**, 2550 (1991).

⁶M. Onoda and T. Inabe, J. Phys. Soc. Jpn. **62**, 2217 (1993).

⁷W. Rudorff and H. Becker, Z. Naturforsch. B **9**, 613 (1954).

⁸B. Reuter, R. Weber, and J. Jaskowski, Z. Elektrochem. **66**, 832 (1962).

⁹R. R. Heikes, R. C. Miller, and R. Mazelsky, Physica **30**, 1600 (1964).

¹⁰J. B. Goodenough and P. M. Racciah, J. Appl. Phys. **36**, 1031 (1965).

¹¹K. Kobayashi, K. Kosuge, and S. Kachi, Mater. Res. Bull. **4**, 95 (1969).

¹²J. B. Goodenough, G. Dutta, and A. Manthiram, Phys. Rev. B **43**, 10 170 (1991).

¹³L. P. Cardoso, D. E. Cox, T. A. Hewston, and B. L. Chamberland, J. Solid State Chem. **72**, 234 (1988).

¹⁴K. Imai *et al.*, J. Solid State Chem. **114**, 184 (1995).

¹⁵J. Kikuchi *et al.*, J. Phys. Soc. Jpn. **60**, 3620 (1991).

¹⁶C. T. Chen and F. Sette, Rev. Sci. Instrum. **60**, 1616 (1989).

¹⁷F. Reinert *et al.*, Z. Phys. B **97**, 83 (1995).

¹⁸A. Manthiram and J. B. Goodenough, Can. J. Phys. **65**, 1309 (1987).

¹⁹C. T. Chen *et al.*, Phys. Rev. Lett. **66**, 104 (1991).

²⁰L. A. de Picciotto and M. M. Thackeray, Mater. Res. Bull. **20**, 187 (1985).

²¹B. T. Thole *et al.*, Phys. Rev. B **31**, 6856 (1985).

²²A. E. Bocquet *et al.*, Phys. Rev. B **53**, 1161 (1996).

²³L. F. Mattheiss, J. Phys. Condens. Mater. **6**, 6477 (1994).

²⁴G. van der Laan *et al.*, Phys. Rev. B **33**, 4253 (1986).

²⁵R. D. Cowan, *The Theory of Atomic Structure and Spectra* (University of California Press, Berkeley, 1981).

²⁶K. Okada *et al.*, Phys. Rev. B **47**, 6203 (1993).

²⁷F. M. F. de Groot *et al.*, Solid State Commun. **927**, 991 (1994).

²⁸S. Sugano, Y. Tanabe, and H. Kamimura, *Multiplets of Transition-Metal Ions in Crystals* (Academic Press, New York, 1970).

²⁹J. Fink *et al.*, Phys. Rev. B **32**, 4899 (1985).

³⁰F. M. F. de Groot *et al.*, Phys. Rev. B **40**, 5715 (1989).

³¹M. Abbate *et al.*, Phys. Rev. B **43**, 7263 (1991).

³²K. I. Kugel and D. I. Khomskii, Zh. Éksp. Teor. Fiz. **64**, 1429 (1973) [Sov. Phys. JETP **37**, 725 (1973)].

³³H. F. Pen *et al.*, Phys. Rev. Lett. **78**, 1323 (1997).